*Progress In Electromagnetics Research Letters, Vol. 92, 1–8, 2020*

# A Design of Crossed Exponentially Tapered Slot Antenna with Multi-Resonance Function for 3G/4G/5G Applications

**Naser O. Parchin[1, *], Haleh J. Basherlou[2], and Raed A. Abd-Alhameed[1]**

**Abstract**—In this research work, a planar crossed exponentially tapered slot antenna with a multi-resonance function is introduced. The presented antenna design is ascertained on a low-cost Rogers 5870 dielectric with a circular schematic. The antenna is designed to support several frequency spectrums of the current and future wireless communications. The configuration of the design contains a pair of crossed exponentially tapered slots intersected by a star-shaped slot in the back layer and a bowtie-shaped radiation stub with a discrete feeding point extended among the stub parts. The crossed exponential slots exhibit a wide impedance, and the star slot generates an extra resonance at the upper frequencies. For $S_{11} \leq -6$, the antenna provides a wide operation band of 1.7 to 5.9 GHz supporting several frequency bands of 3G, 4G, and 5G communication. The fundamental characteristics of the proposed slot radiator are studied, and good performances have been achieved.

## 1. INTRODUCTION

With the rapid development of wireless networks, study and searching for multifunction devices is growing and getting more attention [1–4]. Due to the wide range of wireless applications and a variety of functions, more and more frequency bands are needed to meet these requirements [5–8]. This requires a type of antennas with multi-bands and resonant frequencies and sufficient impedance bandwidth besides high radiation performance [9–13]. Multi-band/multi-resonance antennas have been playing a critical role in modern wireless communication systems since they can support several frequency spectrums for various applications such as up fifth-generation (5G) wireless networks [14–16]. However, 5G is not going to replace 4G, at least not in a short term. Therefore, antenna systems with the capability of supporting not only the required 5G spectrum but also the previous generations are highly demanded [17–19].

In this paper, we introduce a multi-resonance antenna design with a wide spectrum for supporting 3G, 4G, and 5G bands. The designed antenna can support 1900 MHz personal communications service (PCS) of 3G communication, 2.1, 2.3, and 2.5 GHz of 4G networks and different bands of 5G. For the sub-6 GHz spectrum of the upcoming 5G technology, various operation bands including LTE band-42 (3.5 GHz), band-43 (3.7 GHz), band-44 (4 GHz), and band-46 (5.5 GHz) are considered as candidate frequency bands [20–24]. In addition, due to the available RF circuit and test equipment, 2.6 GHz 4G LTE can be considered as a default for future mobile networks and has received many interests recently [25]. Besides, in order to further support more potential sub-6GHz spectrums, LTE band 46 (5.5 GHz), known as Worldwide interoperability for microwave access (WiMAX) operation band, can be considered for 5G massive MIMO [26–28]. The configuration of the presented antenna design is composed of two crossed exponentially tapered slots in the ground plane and a bowtie-shaped radiation stub with a discrete feeding point extended among the stub parts. The antenna supports a wide operation band at 1.8–4.3 GHz with an extra resonance at 5.5 GHz. However, for $S_{11} \leq -6$, the

*Received 23 April 2020, Accepted 27 May 2020, Scheduled 8 June 2020*
* Corresponding author: Naser O. Parchin (n.ojaroudiparchin@bradford.ac.uk).
[1] Faculty of Engineering and Informatics, University of Bradford, Bradford BD7 1DP, UK. [2] Bradford College, Bradford BD7 1AY, UK.

antenna operation band is from 1.7 to 5.9 GHz. It exhibits good properties in terms of the fundamental characteristics and could be used in future wireless communication networks.

## 2. ANTENNA DESIGN AND SCHEMATIC

The front and back views of the antenna configuration are depicted in Fig. 1. The antenna is implemented in a 0.8 mm circular Rogers 5870 dielectric with loss tangent and dielectric constant of 0.0012 and 2.33, respectively. It is a printed planar slot-based antenna, with double-symmetry and balanced con?guration. It contains two crossed exponentially tapered slots, intersected by a star-shaped slot and a bowtie-shaped radiation stub placed at the center of the slots in the top layer. The crossed exponential slots exhibit a wide impedance, and the star slot generates an extra resonance at the upper frequencies. The geometry of the exponential slot is given by

$$w(l) = w_0 \exp(l/C_0) \tag{1}$$

where $w$ is the slot width, and $l$ is the slot longitudinal coordinate. $w_0$ and $C_0$ are the slot width and exponential expansion parameters, respectively. Chopped replicas of two opposing petals of the antenna are printed at the top-side of the substrate. The chopped edge of these petals is an arc of the circumference which creates a bowtie-shaped radiation stub. The feeding point of the antenna is extended among the stub pairs. The CST software is used to investigate the properties designed antenna [29]. More details of design characteristics for this type of antennas can be found in [30, 31]. The values of the antenna design parameters (in mm) are as follows: $W = 37.65$, $R = 30$, $L = 31.25$, $W_1 = 2.15$, $L_1 = 2.7$, $W_2 = 48.4$, $r = 13.5$, $x = 0.5$.

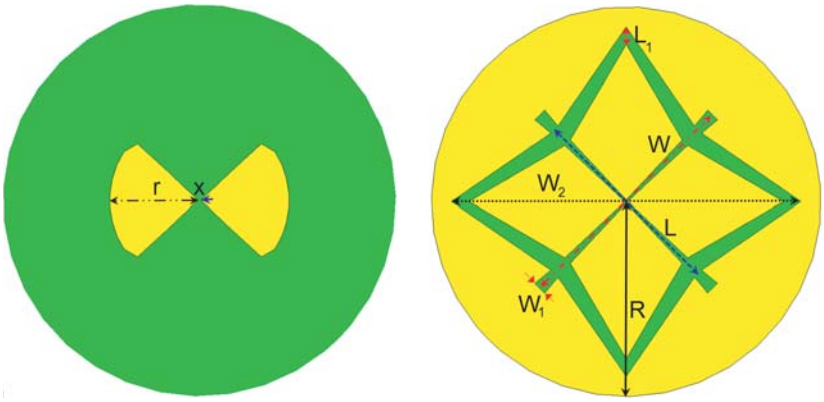


**Figure 1.** (a) Front and (b) back views of the designed antenna.

## 3. CHARACTERISTICS AND RADIATION BEHAVIOR OF THE ANTENNA

The motive behind the proposed antenna design is to achieve a broad impedance bandwidth with multi-resonance function and capability of supporting several frequency bands. This has been obtained by a new antenna design method called crossed exponentially tapered slot antennas. The return loss characteristic of the antenna is shown in Fig. 2(a). As shown, the proposed antenna covers a wide impedance bandwidth at the frequency range of 1.8–4.3 GHz with an extra resonance at 5.5 GHz. Besides, as illustrated, for $S_{11} \leq -6$, the antenna operation band is from 1.7 to 5.9 GHz supporting 1.9 GHz, 2.1 GHz, 2.3 GHz, and 2.5 GHz 4G bands, 2.6 GHz 4G LTE, 3.5 GHz, 3.7 GHz, and 4 GHz of sub 6 GHz, and 5.5 GHz of WiMAX systems [32–34]. The antenna resonates mainly at 1.9 GHz, 4 GHz, and 5.5 GHz, as can be clearly seen from the reflected phase of the design, shown in Fig. 2(b).

To justify the tri-resonance function of the design, the simulated electric field distributions for the proposed antenna at different resonance frequencies are presented in Fig. 3. It is worth mentioning that the maximum scaling for all figures is the same. At the first resonant frequency (1.9 GHz), the maximum

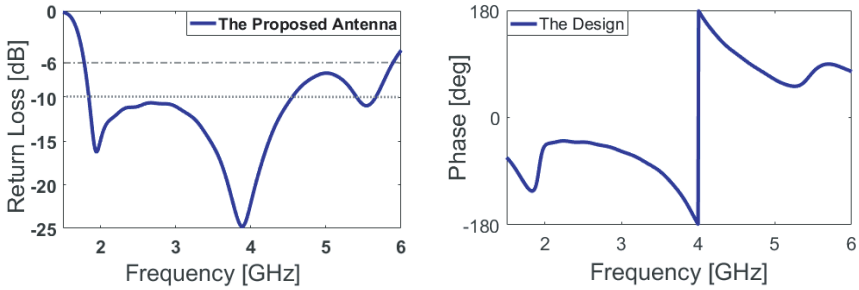


**Figure 2.** (a) Return loss and (b) reflected phase of the proposed antenna.

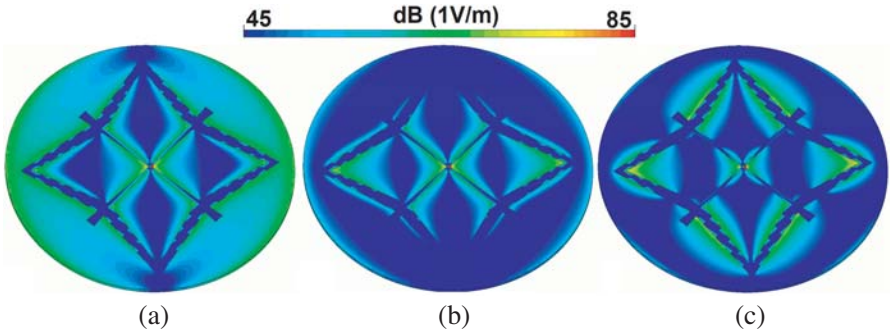


**Figure 3.** Electric field distributions of the proposed antenna at (a) 1.9, (b) 4, and (c) 5.5 GHz.

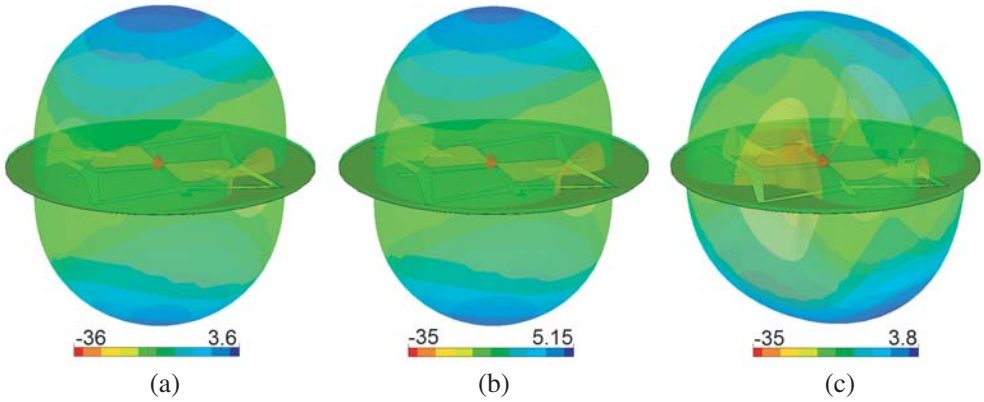


**Figure 4.** 3D transparent radiation patterns at (a) 1.9, (b) 4, and (c) 5.5 GHz.

*E*-filed distributions are discovered at the outside of the crossed exponentially tapered slot [35]. It is evident from Fig. 3(b) that at the second resonance (4 GHz) the star-shaped slot appears very active. As shown in Fig. 3(c), at 5.5 GHz, the electric field distributions are almost equal around different edges of the crossed exponentially tapered slots. Nevertheless, some coupling and interactions between the main slot resonator and the bowtie-shaped radiation stub in the top layer can be discovered which could affect the frequency response of the antenna [36, 37].

The transparent views of the design radiations at different resonance frequencies, including 1.9, 4, and 5.5 GHz, are illustrated in Fig. 4. Clearly, the antenna exhibits highly symmetric radiation patterns covering the different sides of the substrate with sufficient gain values [38, 39]. It should be noted that by moving to the higher frequencies, the shapes of the radiation patterns are changed slightly. Fig. 5(a) plots the simulated radiation and total efficiencies of the antenna. As can be observed from the figure,

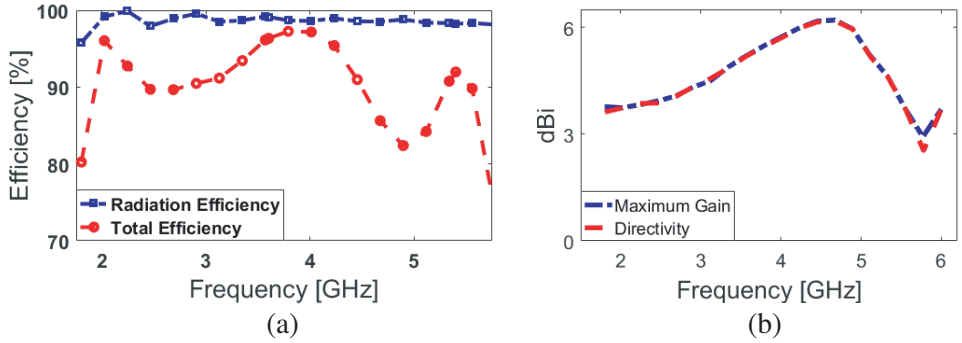


**Figure 5.** (a) Antenna efficiencies (radiation & total) and (b) its maximum gain/diversity characteristics.

better than 95% radiation efficiency is achieved versus the antenna frequency band. Furthermore, it is shown that the designed antenna offers quite good total efficiency with the level of 80% $\sim$ 95% and with the maximum values at the middle frequencies [40–42]. This is mainly due to the good impedance matching and also well-defined characteristics of the employed Rogers 5870 dielectric which is not lossy in comparison with conventional substrates such as FR-4. It should also be noted that the mismatch loss of the antenna is included in the total efficiency characteristic. Therefore, as expected, the total efficiency values are less than the radiation efficiency results. Fig. 5(b) plots the directivity and maximum gain properties of the designed slot antenna versus the desired frequency band. It is found that although the gain changes with the frequency, its level is still better than 3 dBi over the antenna frequency band. The small difference among the maximum gain and directivity characteristics is mainly due to the high-efficiency results at different frequencies [43]. Also, the variation of the directivity and gain is less than 3 dBi which is a good feature for wideband and multi-resonance system applications.

Figure 6(a) illustrates the antenna fabricated prototype and its feeding mechanism. As shown, in the measurements, the inner conductor of a coaxial cable is extended among the stub pairs of the antenna. However, in simulations, a discrete feeding port is extended among the antenna radiation stub pairs [44]. The measured and simulated return loss results of the fabricated sample are compared and represented in Fig. 6(b). It is observed that the fabricated sample of the antenna works properly and exhibits an acceptable agreement with the simulation results. However, a slight variation in the measured return loss is discovered which is due to the feeding setup and the large length of the coaxial cables. As illustrated, a good frequency band ($S_{11} \leq -6$ dB) of 1.7–5.9 GHz is achieved for the fabricated antenna. Also, the 2D radiation patterns are studied for the proposed slot antenna design. The co/cross-pol radiation patterns of the target resonance frequencies, including 1.9, 4, and 5.5 GHz, are represented in Fig. 7. These frequencies are chosen as the lower, middle, and upper resonances, respectively. As seen, the antenna can give dumbbell-like radiations in $E$-plane while omnidirectional radiations are discovered

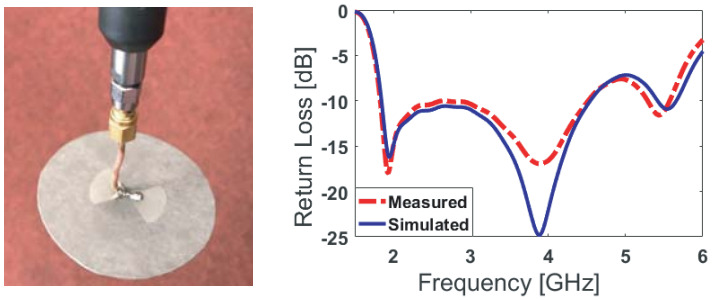


**Figure 6.** The fabricated prototype and the feeding mechanism and (b) measured/simulated return loss results.

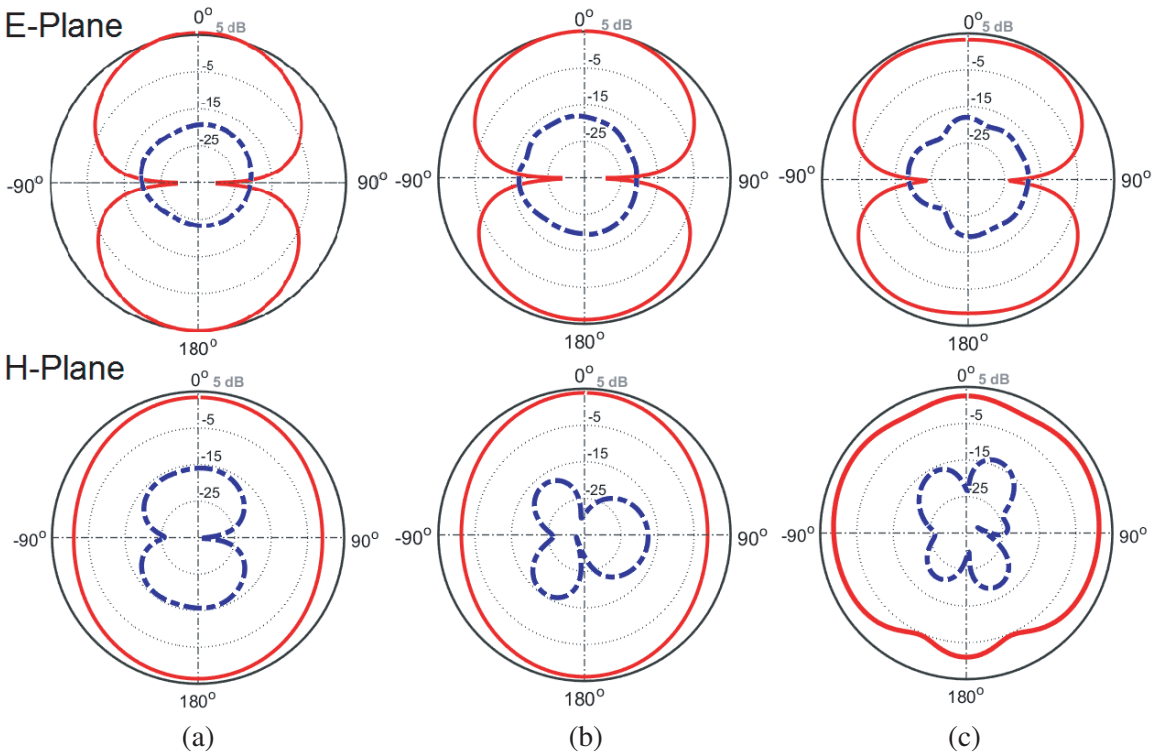


**Figure 7.** Co-pol (solid line) and cross-pol (dashed line) radiation patterns at (a) 1.9 GHz, (b) 4 GHz, and (c) 5.5 GHz.

in $H$-plane. With increasing the operation frequency, the antenna radiations are slightly deteriorated. In addition, the cross-polarizations of the antenna radiation can be deteriorated due to the horizontal surface currents. However, as clearly shown, the antenna provides good cross-polarization radiation patterns with low levels at different frequencies [45–48].

In the following, the mutual coupling characteristics between the antenna pairs for three different MIMO configurations are investigated. In this investigation, the closely-spaced antennas are arranged on a common dielectric with a minimum distance. The results are compared and illustrated in Fig. 8. As can be observed, the crossed arrangement (configuration 3) provides the best mutual coupling and isolation. This is mainly due to the independent orthogonal polarization modes of the antenna elements which have been arranged with a 90° difference [49, 50]. However, configuration 2 is also quite satisfactory with the mutual coupling less than −20.

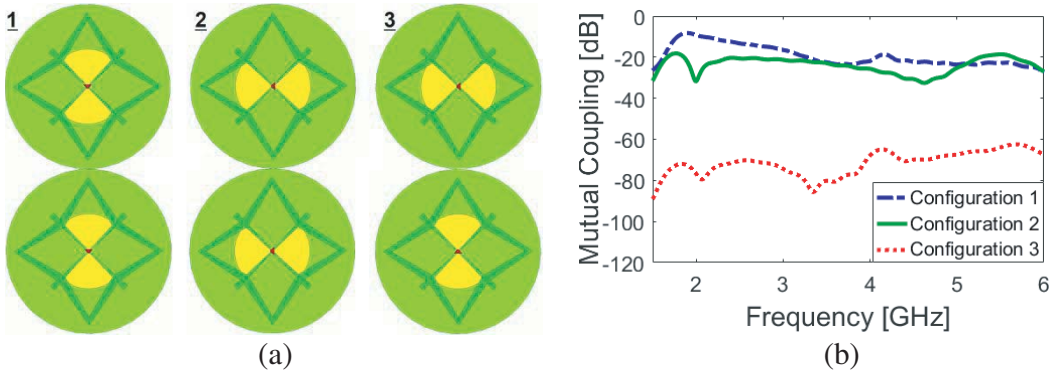


**Figure 8.** (a) Different arrangements and (b) mutual coupling results of the double-antenna.

## 4. CONCLUSION

The design and characteristics of a new multi-resonance crossed exponentially tapered slot antenna is successfully investigated in this paper. The structure of the designed antenna contains two crossed exponentially tapered slots in the ground plane and a bowtie-shaped radiation stub with a discrete feeding point extended among the stub parts. The antenna supports a wide operation band at 1.8–4.3 GHz with an extra resonance at 5.5 GHz. The fabricated prototype sample of the design works properly and exhibits an acceptable agreement with the simulation results. It exhibits good properties in terms of the fundamental radiation characteristics and could be used in future wireless systems.

## ACKNOWLEDGMENT

This project has received funding from the European Union's Horizon 2020 research and innovation programme under grant agreement H2020-MSCA-ITN-2016 SECRET-722424.

## REFERENCES

1. Kumar, G. and K. P. Ray, *Broadband Microstrip Antennas*, Artech House Inc., Norwood, MA, 2003.
2. Salonen, P., et al., "A small planar inverted-F antenna for wearable applications," *IEEE International Symposium on Wearable Computers*, 96–100, 1999.
3. Ojaroudi, M., et al., "Dual band-notch small square monopole antenna with enhanced bandwidth characteristics for UWB applications," *ACES Journal*, Vol. 25, 420–426, 2012.
4. Al-Yasir, Y. I. A., et al., "A new polarization-reconfigurable antenna for 5G applications," *Electronics*, Vol. 7, 293, 2018.
5. Ojaroudi, N. and N. Ghadimi, "Dual-band CPW-fed slot antenna for LTE and WiBro applications," *Microw. Opt. Technol. Lett.*, Vol. 56, 1013–1015, 2014.
6. Ojaroudiparchin, N., M. Shen, and G. F. Pedersen, "Investigation on the performance of low-profile insensitive antenna with improved radiation characteristics for the future 5G applications," *Microw. Opt. Technol. Lett.*, Vol. 58, 2148–2158, 2016.
7. Parchin, N. O., et al., "Recent developments of reconfigurable antennas for current and future wireless communication systems," *Electronics*, Vol. 8, 128, 2019.
8. Ojaroudi, N., et al., "An omnidirectional PIFA for downlink and uplink satellite applications in C-band," *Microwave and Optical Technology Letters*, Vol. 56, 2684–2686, 2014.
9. Ojaroudi, N. and N. Ghadimi, "Design of CPW-fed slot antenna for MIMO system applications," *Microw. Opt. Technol. Lett.*, Vol. 56, 1278–1281, 2014.
10. Ren, Z., S. Wu, and A. Zhao, "Triple band MIMO antenna system for 5G mobile terminals," *2019 International Workshop on Antenna Technology (iWAT)*, 163–165, Miami, FL, USA, 2019.
11. Ojaroudiparchin, N., M. Shen, and G. F. Pedersen, "$8 \times 8$ planar phased array antenna with high efficiency and insensitivity properties for 5G mobile base stations," *EuCAP 2016*, 1–5, Davos, Switzerland, 2016.
12. Parchin, N. O. and R. A. Abd-Alhameed, "A compact Vivaldi antenna array for 5G channel sounding applications," *EuCAP*, London, UK, 2018.
13. Ojaroudi Parchin, N., H. J. Basherlou, and R. A. Abd-Alhameed, "Dual circularly polarized crescent-shaped slot antenna for 5G front-end systems," *Progress In Electromagnetics Research Letters*, Vol. 91, 41–48, 2020.
14. Ojaroudi, N., H. Ojaroudi, and N. Ghadimi, "Quadband planar inverted-F antenna (PIFA) for wireless communication systems," *Progress In Electromagnetics Research Letters*, Vol. 45, 51–56, 2014.
15. Hussain, R., et al., "Compact 4G MIMO antenna integrated with a 5G array for current and future mobile handsets," *IET Microw. Antennas Propag.*, Vol. 11, 271–279, 2017.

16. Parchin, N. O., et al., "A radiation-beam switchable antenna array for 5G smartphones," *2019 PhotonIcs & Electromagnetics Research Symposium — Fall (PIERS — FALL)*, 1769–1774, Xiamen, China, Dec. 17–20, 2019.
17. Parchin, N. O., et al., "Microwave/RF components for 5G front-end systems," *Avid Science*, 1–200, 2019.
18. Parchin, N. O., "Multi-band MIMO antenna design with user-impact investigation for 4G and 5G mobile terminals," *Sensors*, Vol. 19, 456, 2019.
19. Parchin, N. O., et al., "Dual-polarized multi-antenna system for massive MIMO cellular communications," *International Journal of Information and Communication Engineering*, Vol. 14, 140–144, 2020.
20. Gozalvez, J., "5G worldwide developments [mobile radio]," *IEEE Veh. Technol. Mag.*, Vol. 12, 4–11, 2017.
21. Bonfante, A., et al., "5G massive MIMO architectures: self-backhauled small cells versus direct access," *IEEE Transactions on Vehicular Technology*, Vol. 68, 10003–10017, 2019.
22. "5G in the Sub-6 GHz spectrum bands," [Online], Available: http://www.rcrwireless.com/20160815/fundamentals/5g-sub-6ghztag31-tag99.
23. 5G NR (New Radio), Accessed: Dec. 12, 2018, [Online], Available: http://3gpp.org/.
24. Parchin, N. O., et al., "A substrate-insensitive antenna array with broad bandwidth and high efficiency for 5G mobile terminals," *2019 PhotonIcs & Electromagnetics Research Symposium — Fall (PIERS — FALL)*, 1764–1768, Xiamen, China, Dec. 17–20, 2019.
25. Parchin, N. O., et al., "High-performance Yagi-Uda antenna array for 28 GHz mobile communications," *23th Telecommunications Forum, TELFOR 2019*, Belgrade, Serbia, Nov. 25–27, 2019.
26. Parchin, N. O., et al., "Eight-port MIMO antenna system for 2.6 GHz LTE cellular communications," *Progress In Electromagnetics Research C*, Vol. 99, 49–59, 2020.
27. Basherlou, H. J., et al., "MIMO monopole antenna design with improved isolation for 5G WiFi applications," *International Journal of Electrical and Electronic Science*, Vol. 7, 1–5, 2019.
28. Parchin, N. O., et al., "Frequency reconfigurable antenna array with compact end-fire radiators for 4G/5G mobile handsets," *IEEE 2nd 5G World Forum (5GWF)*, Dresden, Germany, 2019.
29. *CST Microwave Studio*, ver. 2018, CST, Framingham, MA, USA, 2018.
30. Costa, J. R. and C. A. Fernandes, "Broadband slot feed for integrated lens antennas," *IEEE Antennas and Wireless Propagation Letters*, Vol. 6, 396–400, 2007.
31. Costa, J. R. and C. A. Fernandes, "Crossed exponentially tapered slot antenna for UWB applications," *2008 IEEE Antennas and Propagation Society International Symposium*, 1–4, San Diego, CA, 2008.
32. Valizade, A., et al., "CPW-fed small slot antenna with reconfigurable circular polarization and impedance bandwidth characteristics for DCS/WiMAX applications," *Progress In Electromagnetics Research C*, 65–72, 2015.
33. Ojaroudi, N., et al., "Enhanced bandwidth of small square monopole antenna by using inverted U-shaped slot and conductor-backed plane," *Applied Computational Electromagnetics Society (ACES)*, Vol. 27, 685–690, 2012.
34. Valizade, A., et al., "Band-notch slot antenna with enhanced bandwidth by using Ω-shaped strips protruded inside rectangular slots for UWB applications," *Appl. Comput. Electromagn. Soc. (ACES) J.*, Vol. 27, 816–822, 2012.
35. Costa, J. R., C. R. Medeiros, and C. A. Fernandes, "Performance of a Crossed Exponentially Tapered Slot Antenna for UWB Systems," *IEEE Transactions on Antennas and Propagation*, Vol. 57, No. 5, 1345–1352, May 2009.
36. Jamesn, J. R., and P. S. Hall, *Handbook of Microstrip Antennas*, Peter Peregrinus Ltd., London, 1989.
37. Ojaroudi, N., "Circular microstrip antenna with dual band-stop performance for ultra-wideband systems," *Microw. Opt. Technol. Lett.*, Vol. 56, 2095–2098, 2014.

38. Parchin, N. O., et al., "Reconfigurable phased array 5G smartphone antenna for cognitive cellular networks," *23th Telecommunications Forum, TELFOR 2019*, Belgrade, Serbia, Nov. 25–27, 2019.
39. Parchin, N. O., et al., "UWB mm-wave antenna array with quasi omnidirectional beams for 5G handheld devices," *IEEE International Conference on Ubiquitous Wireless Broadband (ICUWB)*, Nanjing, China, 2016.
40. Ojaroudi, N., et al., "Compact ultra-wideband monopole antenna with enhanced bandwidt-hand dual band-stop properties," *International Journal of RF and Microwave Computer-AidedEngineering*, 346–357, 2014.
41. Parchin, N. O., et al., "MM-wave phased array Quasi-Yagi antenna for the upcoming 5G cellularcommunications," *Applied Sciences*, Vol. 9, 1–14, 2019.
42. Parchin, N. O., H. J. Basherlou, and R. A. Abd-Alhameed, "UWB microstrip-fed slot antenna with improved bandwidth and dual notched bands using protruded parasitic strips," *Progress In Electromagnetics Research C*, Vol. 101, 261–273, 2020.
43. Musavand, A., et al., "A compact UWB slot antenna with reconfigurable band-notched functionfor multimode applications," *Applied Computational Electromagnetics Society (ACES) Journal*, Vol. 13, No. 1, 975–980, 2016.
44. Parchin, N. O., "Low-profile air-filled antenna for next generation wireless systems," *Wireless Personal Communications*, Vol. 97, 3293–3300, 2017.
45. Mazloum, J., A. Ghorashi, M. Ojaroudi, and N. Ojaroudi, "Compact triple-band S-shaped monopole diversity antenna for MIMO applications," *Appl. Comput. Electromagn. Soc. J.*, Vol. 30, 975–980, 2015.
46. Elfergani, I. T. E., A. S. Hussaini, J. Rodriguez, R. Abd-Alhameed, *Antenna Fundamentals for Legacy Mobile Applications and Beyond*, 1–659, Springer, Switzerland, 2017.
47. Ojaroudi, N., "Design of microstrip antenna for 2.4/5.8 GHz RFID applications," *German Microwave Conference, GeMic 2014*, RWTH Aachen University, Germany, Mar. 10–12, 2014.
48. Siahkal-Mahalle, B. H., et al., "Enhanced bandwidth small square monopole antenna with band-notched functions for UWB wireless communications," *Applied Computational Electromagnetics Society (ACES) Journal*, 759–765, 2012.
49. Parchin, N. O., et al., "A closely spaced dual-band MIMO patch antenna with reduced mutual coupling for 4G/5G applications," *Progress In Electromagnetics Research C*, Vol. 101, 71–80, 2020.
50. Parchin, N. O., et al., "Design of multi-mode antenna array for use in next-generation mobile handsets," *Sensors*, Vol. 20, 2447, 2020.